A novel harmonic current sharing control strategy for parallel-connected inverters

Guan, Yajuan; Guerrero, Josep M.; Savaghebi, Mehdi; Quintero, Juan Carlos Vasquez; Wei, Feng

A Novel Harmonic Current Sharing Control Strategy for Parallel-Connected Inverters

Yajuan Guan, Josep M. Guerrero, Mehdi Savaghebi, Juan C. Vasquez

Microgrid Research Programme www.microgrids.et.aau.dk
Department of Energy Technology
Aalborg University, Denmark
{ygu, joz, mes, juq}@et.aau.dk

Wei Feng

Department of Electrical Engineering
Tsinghua University
Beijing, China
fwqqrse@163.com

Abstract— **A novel control strategy which enables proportional linear and nonlinear loads sharing among paralleled inverters and voltage harmonic suppression is proposed in this paper. The proposed method is based on the autonomous currents sharing controller (ACSC) instead of conventional power droop control to provide fast transient response, decoupling control and large stability margin. The current components at different sequences and orders are decomposed by a multi-second-order generalized integrator-based frequency locked loop (MSOGI-FLL). A harmonic-orthogonal-virtual-resistances controller (HOVR) is used to proportionally share current components at different sequences and orders independently among the paralleled inverters. Proportional resonance controllers tuned at selected frequencies are used to suppress voltage harmonics. Simulations based on two 2.2 kW paralleled three-phase inverters are carried out to validate the performance of the proposed method.**

Keywords—*harmonic current sharing; ACSC; droop control; MSOGI-FLL*

Fig. 1. Overall scheme of an islanded microgrid.

I. INTRODUCTION

The islanded microgrid (MG) powered by batteries and renewable energy sources can be deployed to alleviate the power shortage pressure, as shown in Fig.1. However, the increasing usage of power electronics-based interfacing inverters for distributed generation (DG) units will result in harmonic interaction and even lead to resonances in MG. In addition, the presences of nonlinear loads, passive harmonic filters, and parasitic capacitors in distribution feeders, induce harmonic current and low order harmonic resonance [1]-[4].

In order to maintain the harmonic components of the voltage output within the required limitation, and to share the harmonic currents among the paralleled voltage controlled inverters (VCIs), a number of investigations have been conducted to address these challenges. In [5], a droop control based on the reactive volt-ampere consumption of harmonics of each interface converter is proposed. The G–H and Q–G droop controls were employed to share harmonics and unbalanced currents among DG units in islanded MGs in [6]. An enhanced harmonic current sharing approach is discussed in [7]. The virtual impedances at fundamental and harmonic frequencies are regulated using DG line current and point of common coupling voltage feed-forward terms. Therefore, the impacts of mismatched physical feeder impedances are compensated, and better reactive and harmonic power sharing are realized.
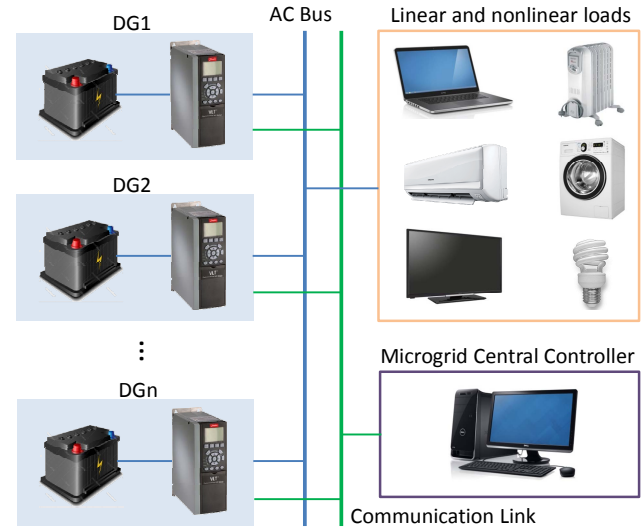
A power-harmonic conductance droop was proposed in [8]. However, since the RMS values of total active and reactive harmonic power were used, harmonic components at different sequences and orders cannot be controlled separately.

Communication-based approaches for harmonic current sharing improvement have been reported. In [9], the harmonic compensation was calculated using a secondary controller and then sent to VCIs at the primary level. A voltage waveform control approach for suppressing harmonics was proposed in [10] to achieve harmonic voltage redistribution process in an islanded microgrid.

However, these aforementioned harmonic current sharing control strategies were all developed based on power droop control, which has small stability margin and relatively slow transient response mainly caused by low-pass filters. Therefore a novel simple and effective autonomous current-sharing controller (ACSC) for paralleled three-phase VCIs is proposed in [11]. A control structure consists of a synchronous-reference-frame virtual resistance (SRF-VR) loop and an SRF-based phase-locked loop (SRF-PLL) are used to replace the conventional droop controller in order to obtain faster response and more accurate power sharing performance. However, the control principle discussed in [11] is only related to the fundamental current sharing.

In order to deal with harmonic current sharing, an ACSC based new control strategy is investigated in this paper, thereby the decoupled current sharing performance and stability margin is maintained. Moreover, a multi-second-order generalized integrator based frequency-locked-loop (MSOGI-FLL) is used to decompose current components at different sequences and orders. A harmonic-orthogonal-virtual-resistances (HOVR) controller is adopted to improve harmonic current-sharing performance. The proportional resonance (PR) controllers tuned at selected frequencies in voltage control loops are used to suppress voltage harmonics. Finally, the load currents at different sequences and orders among the paralleled VCIs can be shared proportionally and independently. A simulation model consists of two improved ACSC-based VSIs and a nonlinear load is established in Simulink/Matlab to validate the performance of the proposed control strategy.

II. CONVENTIONAL ACSC STRUCTURE REVIEW

The conventional ACSC is used to control VCIs to proportionally share the load current among the paralleled VCIs instead of the well-known droop controller, as shown in Fig. 2 [11]. A SRF-PLL is used for calculating the phase angular of voltage output. The voltage reference V_{ref} is generated by combining the constant amplitude reference ($\left|V_{ref}\right|$) and the phase angular (θ) generated by the SRF-PLL. The PR-based inner voltage and current controllers ($G_v(s)$ and $G_i(s)$) are adopted in $\alpha\beta$ reference frame. The current output of each VCI (i_{odq}) is transformed to the SRF. The current outputs in dq reference frame are independently controlled by SRF-VR loop. The closed loop transfer function of the system can be described as follows:

$$
\begin{aligned}
T_{plant}(s) &= \frac{V_o(s)}{V_{ref}(s)} \\
&= \frac{G(s)\left[1+G_{Lequ}(s)Z_{line}(s)\right]}{1+G_{Lequ}(s)Z_{line}(s)+G_{vir}(s)G(s)+G_{Lequ}(s)Z_o(s)}
\end{aligned}
\tag{1}
$$

where $G(s)$ presents the tracking performance of the output voltage following voltage reference, $Z_o(s)$ is the equivalent output impedance of the inverter, $Z_{line}(s)$ is the line impedance, $G_{Lequ}(s)$ is the equivalent load admittance, $G_{vir}(s)$ is equal to $R_{vird}/R_{Lequ}+R_{virq}/sL_{Lequ}$.

When supplying active loads with resistance line impedance, the d-axis current flowing through the SRF-VR will drop the direct voltage, causing a decrease in the output voltage amplitude. Hence, a droop characteristic is imposed by adapting the voltage output amplitude according to SRF-VR, which endows the $I_{od}-V$ droop characteristic to the system. Meanwhile, even though the SRF-PLL is trying to synchronize the inverter with common AC bus, in the case of supplying reactive loads, the q-axis current flowing through the SRF-VR will produce an unavoidable quadrature voltage drop, which will cause an increase in SRF-PLL frequency. Thus, the
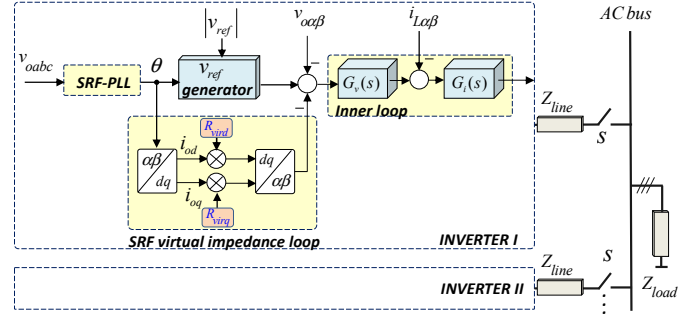

Fig. 2. Control structure of a VCI with conventional ACSC.

mechanism inherently endows an $I_{oq}-\omega$ droop characteristic in each inverter.

The relationships of I_{od}, I_{oq}, R_{vird} and R_{virq} can be expressed for number N of converters as shown in 2(a) and 2(b). The current outputs I_{od} and I_{oq} of the VCIs are inversely proportional to the corresponding SRF-VR. Therefore, the current outputs in dq reference frame of each VCI can be regulated independently.

$$I_{od1}R_{vird1} = I_{od2}R_{vird2} = \cdots = I_{odN}R_{virdN} \tag{2a}$$

$$I_{oq1}R_{virq1} = I_{oq2}R_{virq2} = \cdots = I_{oqN}R_{virqN} \tag{2b}$$

As the parallel-VCIs should be stable at the cross zero point of the phase-frequency characteristic based on (1), the relationship of R_{virq}, I_{oq} and ω can be obtained by presetting R_{vird} and I_{od} to fixed values. The relationship of R_{virq}, I_{oq} and ω with zero line impedances is shown in Figs. 3-4.
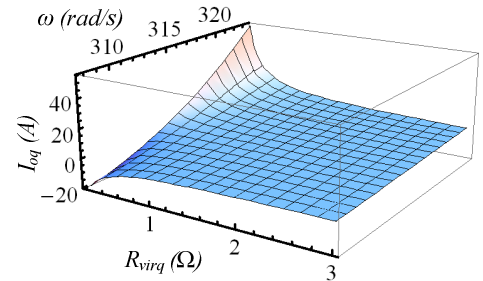

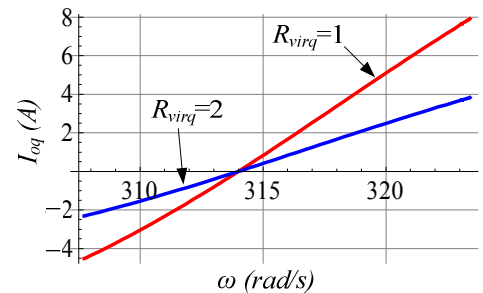Fig. 3. Relationship of R_{virq}, I_{oq} and ω (conventional ACSC).

Fig. 4. Relationship of I_{oq} and ω with fixed R_{virq} (conventional ACSC).
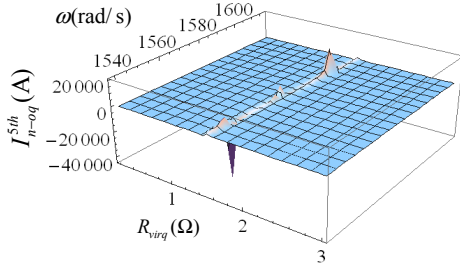
Fig. 5. Relationship of R_{virq}, I_{oq}^{5th} and ω (conventional ACSC).
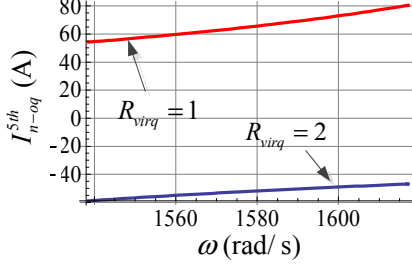

Fig. 6. Relationship of I_{n-oq}^{5th} and ω with fixed R_{virq} (conventional ACSC).

III. PROPOSED ACSC-BASED HARMONIC CURRENT SHARING CONTRTOL STRATEGY

Even though the conventional ACSC-based VCI is properly designed to maintain the stable operation of fundamental voltage frequency/magnitude and to share the fundamental d- and q-axis current outputs according to the SRF-VR ratio, the proportional harmonic current components sharing among the paralleled VCIs cannot be guaranteed. Fig. 5 shows the relationship of R_{virq}, I_{oq}^{5th} and ω at 5th harmonic frequency. It can be seen that as the R_{virq} or ω changing, the I_{oq}^{5th} has non-linear and huge changes. Similarly, the relationship between I_{oq}^{5th} and ω can be derived when R_{virq} is preset to fixed values, as shown in Fig. 6. In order to overcome this problems, three main improvements including the fundamental frequency estimation, the harmonic current decomposition and the proposed HOVR, are added to the ACSC control strategy.

A. Phase estimation with distorted voltage

When supplying the nonlinear loads in an islanded MG with ACSC-based VCIs, the inevitable distorted voltage output resulting from the harmonic equivalent impedance of VCIs and the insufficient harmonic current supply capability will influence the fundamental phase estimation of the regular SRF-PLL, thereby deteriorating the stability of the paralleled VCIs. Therefore, a notch filter, as described in (3), is adopted to abstract the fundamental voltage component from the distorted VCI voltage output.

$$G_{notch}(s) = \frac{n_{notch}s}{s^2 + n_{notch}s + \omega_b^2} \quad (3)$$

where ω_b is the fundamental angular frequency, the attenuation performance of the notch filter can be adjusted by regulating n_{notch}, as presented in Fig. 7.
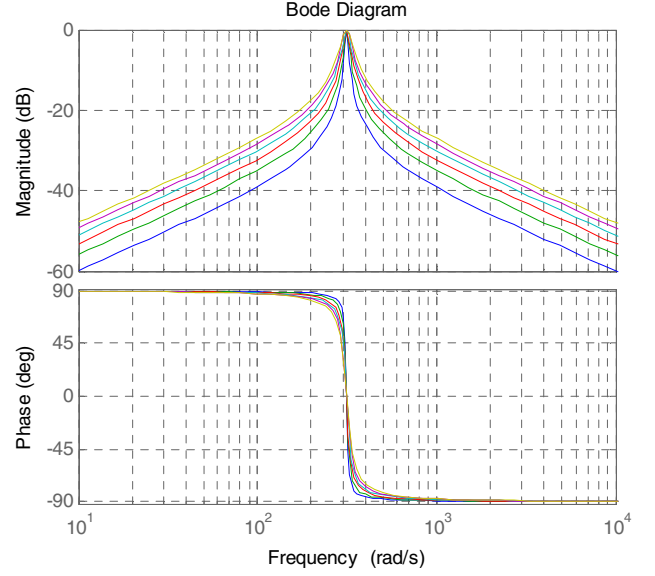

Fig. 7. Bode diagram of the adopted notch filter.

B. Harmonic current components decomposition

It can be seen from Fig. 8 that a MSOGI-FLL is adopted to decompose the VCI current output into different sequences and orders orthogonally. SOGI controllers with different orders are used to calculated the corresponding orthogonal current components ($I_{\alpha\beta}^{ith}$ and $qI_{\alpha\beta}^{ith}$), as follows:

$$D^{ith}(s) = \frac{k_{SOGI}\omega_i s}{s^2 + k_{SOGI}\omega_i s + \omega_i^2} \quad (4)$$

$$Q^{ith}(s) = \frac{k_{SOGI}\omega_i^2}{s^2 + k_{SOGI}\omega_i s + \omega_i^2} \quad (5)$$

Where ω_i is the harmonic angular frequency calculated by SOGI-based FLL, k_{SOGI} is used to adjust the dynamic performance of SOGI. $I_{\alpha\beta}^{ith}$ is used as the feedback of harmonic decoupling network (HDN) to abstract the current components at different orders from sampled current output $I_{\alpha\beta}$ in the stationary reference frame, as shown in (6).

$$I_{\alpha\beta}^{ith} = I_{\alpha\beta} - \sum_{n \neq i} I_{\alpha\beta}^{nth} \quad (6)$$

A positive-negative-sequence calculation block (PNSC) is used to decompose different sequence components ($I_{pn-\alpha\beta}^{ith}$) from $I_{\alpha\beta}^{ith}$ and $qI_{\alpha\beta}^{ith}$, which can be expressed as follows:

$$\begin{cases} I_{p-\alpha}^{ith} = \frac{1}{2}(I_{\alpha}^{ith} - qI_{\beta}^{ith}) \\ I_{p-\beta}^{ith} = \frac{1}{2}(qI_{\alpha}^{ith} + I_{\beta}^{ith}) \end{cases} \quad (7)$$

$$\begin{cases} I_{n-\alpha}^{ith} = \frac{1}{2}(I_{\alpha}^{ith} + qI_{\beta}^{ith}) \\ I_{n-\beta}^{ith} = \frac{1}{2}(-qI_{\alpha}^{ith} + I_{\beta}^{ith}) \end{cases} \quad (8)$$
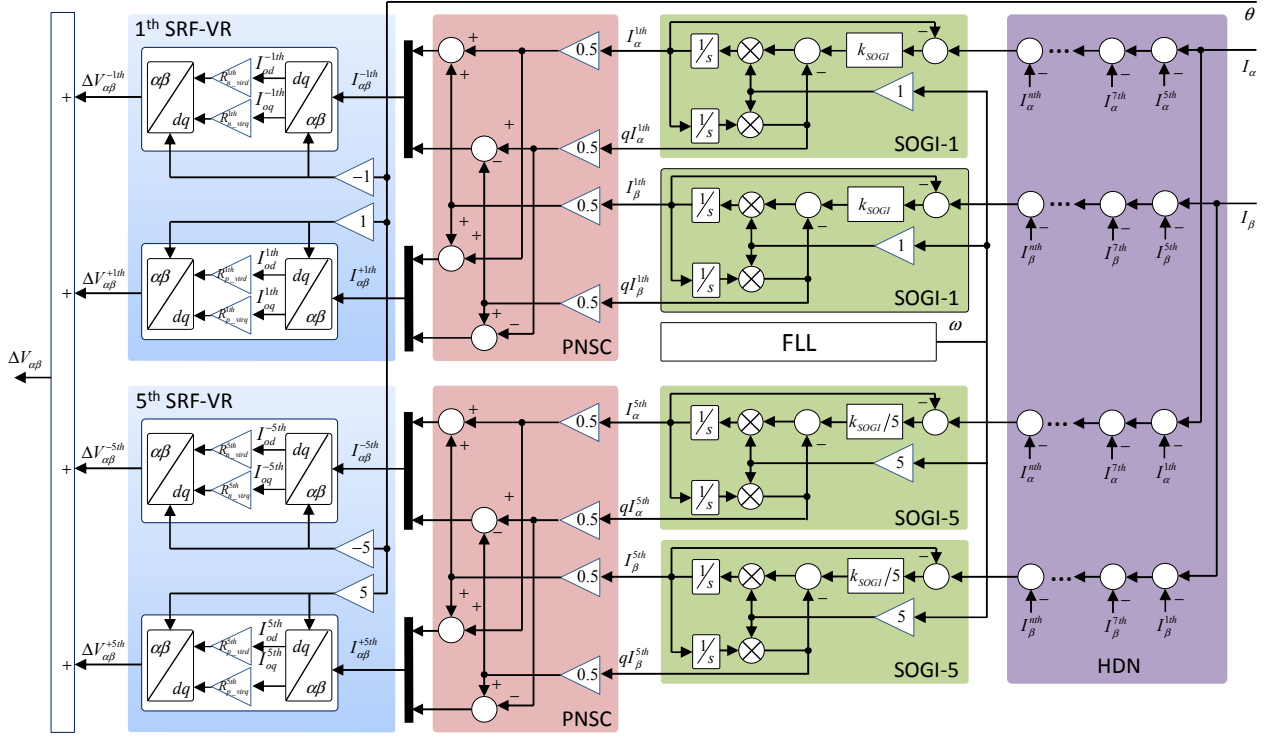
Fig. 8. Overview of the proposed control scheme.

The resonant frequency (ω_i) of SOGI is estimated by SOGI-based FLL, in which the gain r_{FLL} is used to adjust its dynamic performance.

C. Proposed HOVR

Since the SRF-VR loop will influence the frequency and magnitude at zero phase delay point based on the VCI's transfer function, the fundamental d- and q-axis current outputs can be shared among the original ACSC-based VCIs. The same control principle can be implemented to share the harmonic current outputs among the VCIs. The decomposed current components in the stationary reference frame ($I_{\alpha\beta}^{ith}$) are firstly transferred to the dq reference frame with corresponding angular frequency at specific sequences and orders. Then positive and negative harmonic SRF-VRs ($R_{pn-virdq}^{ith}$) are adopted, as shown in Fig. 8, to share the harmonic current independently. The direct and quadrature voltage drops (ΔV_{dq}^{ith}) at different sequences and orders are transferred back to the stationary reference frame ($\Delta V_{\alpha\beta}^{ith}$). The final voltage drop can be calculated as follows:

$$\Delta V_{\alpha\beta} = \sum_{i=\pm1,\pm5...} \Delta V_{\alpha\beta}^{ith} \qquad (9)$$

As the harmonic voltage drop is added to the original three-phase voltage reference, the harmonic RP voltage controllers are used for improving harmonic current output capability. In this sense, the different orders of positive and negative components of d-axis and q-axis output current components
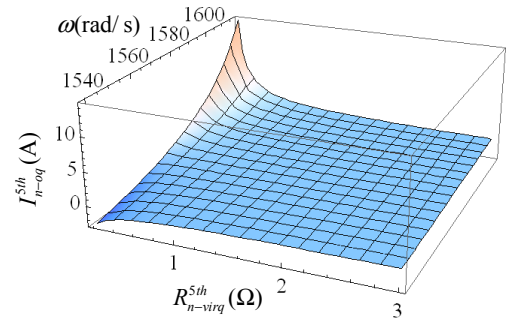
Fig. 9. Relationship of R_{n-virq}^{5th}, I_{n-oq}^{5th} and ω (improved ACSC)
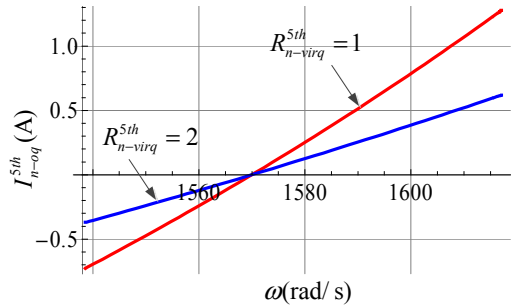

Fig. 10. Relationship of I_{n-oq}^{5th} and ω with fixed R_{n-virq}^{5th} (improved ACSC)

can be shared according to the ratio of $R_{pn-virdq}^{ith}$ in HOVR respectively. The relationship can be represented as follow:

$$I_{p-odq1}^{ith} R_{p-virdq1}^{ith} = I_{p-odq2}^{ith} R_{p-virdq2}^{ith} = ... I_{p-odqn}^{ith} R_{p-virdqn}^{ith} , \quad i = 3k+1$$
$$I_{n-odq1}^{ith} R_{n-virdq1}^{ith} = I_{n-odq2}^{ith} R_{n-virdq2}^{ith} = ... I_{n-odqn}^{ith} R_{n-virdqn}^{ith} , \quad i = 3k+2 \quad (10)$$

The inherent harmonic current sharing principle is similar to the fundamental analysis of original ACSC, the relationship between I_{n-oq}^{5th}, ω and R_{n-virq}^{5th} can be derived from (11), as shown in Fig. 9. The relationship between I_{n-oq}^{5th} and different R_{n-virq}^{5th} can be derived, as shown in Fig. 10. It can be seen that the gradient of the curve is changed according to different R_{n-virq}^{5th}, which means the corresponding current component can be shared proportionally.

$$arc \tan \left[T_{plant}(j\omega) \right] = 0° \Big|_{\omega \subset (1500,1600)} \quad (11)$$

IV. SIMULATION VERIFICATION

To verify the validity of the proposed harmonic current sharing control strategy, a simulation model is established in Simulink/Matlab, which includes two improved ACSC-based VCIs, local linear loads and a rectifier-based nonlinear load. The positive and negative sequences of 5th, 7th and 11th harmonic current components are taken into consideration. The detailed parameters of the simulation model are shown in Tables. I and II.

The simulation results of the proposed controller are shown in Figs. 11 and 12. At the beginning, DG #1 and DG #2 operate in parallel supplying a 3 kW linear load. At 1 s, a nonlinear load is connected to the common AC bus. The dynamic response is around 0.1 s. The ratio of the positive d-axis VR for 1th and 7th harmonic current components is 1:2, while the negative d-axis VR ratio for 5th and 11th harmonic current components is 2:1. The ratio of positive q-axis VR for 1th and 7th is 2:1, while the negative q-axis VR ratio for 5th and 11th is 1:2. As shown in Figs. 11 and 12, the different orders of positive and negative components of orthogonal currents can be shared according to their corresponding VR ratios.

TABLE I
CONTROL PARAMETERS OF SIMULATION

	Parameters		Value
	Symbol	Description	
Electrical Circuit	V_{dc}	DC Voltage	650 V
	V_{MG}	MG Voltage	311 V
	f	Grid Frequency	50 Hz
	L_f	Filter Inductance	1.8 mH
	C_f	Filter Capacitance	9.9 μF
Loads	P_{linear}	P of linear load	3000 W
	Q_{linear}	Q of linear load	0 Var
Loads	$R_{nonlinear}$	Load of rectifier bridge	40 Ω
	$C_{nonlinear}$	Filter of rectifier bridge	50uF
Inner Loops	k_{pv}	Voltage proportional term	0.04
	k_{iv}^{1th}	1th Voltage resonant term	93.839
	k_{iv}^{5th}	5th Voltage resonant term	50
	k_{iv}^{7th}	5th Voltage resonant term	20
	k_{iv}^{11th}	5th Voltage resonant term	100
	k_{pi}	Current proportional term	0.07
	k_{pPLL}	PLL proportional term	1.4
	k_{iPLL}	PLL integral term	2000
	k_{SOGI}	Proportional term for SOGI	2.8
	r_{FLL}	Proportional term for FLL	-1
	n_{notch}	Attenuation parameter for notch	15

TABLE III
VIRTUAL RESISTANCES OF VCIS

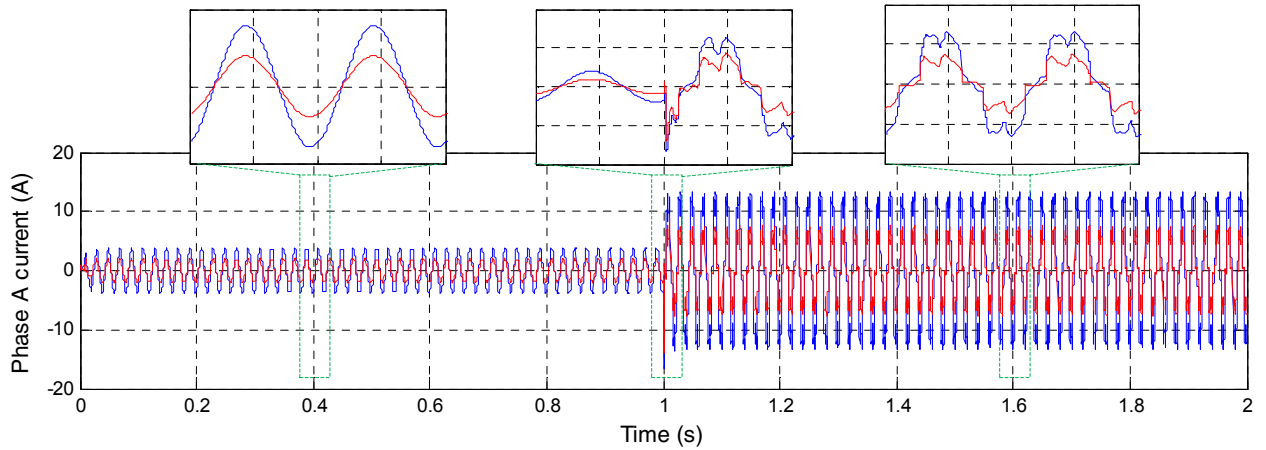|	Order	VCI #1		VCI #2	
		Positive	Negative	Positive	Negative
Direct	1th	4 Ω	2 Ω	2 Ω	4 Ω
	5th	6 Ω	3 Ω	3 Ω	6 Ω
	7th	6 Ω	3 Ω	3 Ω	6 Ω
	11th	6 Ω	3 Ω	3 Ω	6 Ω
Quadrature	1th	2 Ω	4 Ω	4 Ω	2 Ω
	5th	3 Ω	6 Ω	6 Ω	3 Ω
	7th	3 Ω	6 Ω	6 Ω	3 Ω
	11th	3 Ω	6 Ω	6 Ω	3 Ω

Fig. 11 Simulation results of the current outputs (phase a) of the two VCIs.
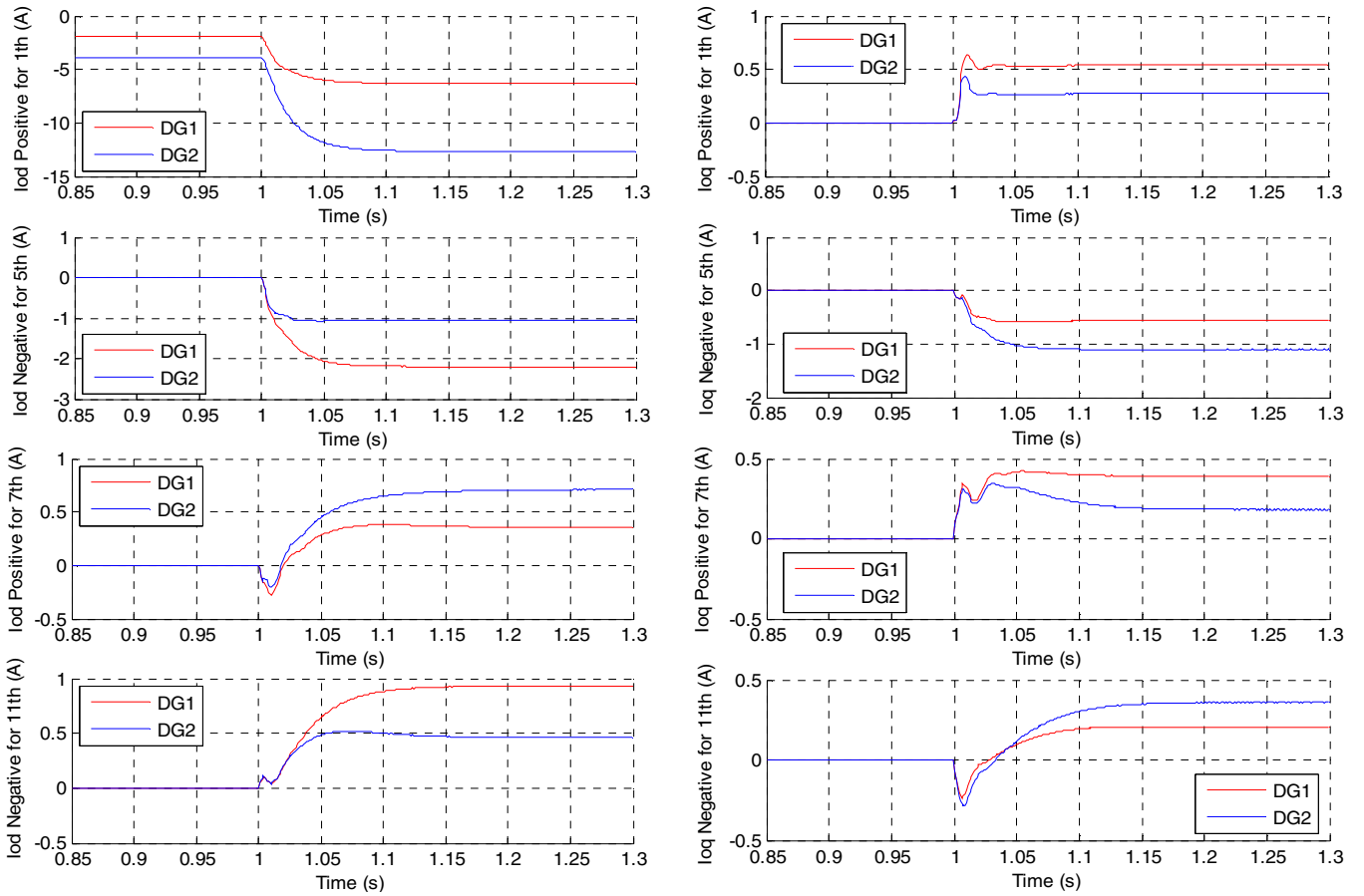
Fig. 12 Simulation results of sharing positive and negative harmonic currents with the proposed controller.

V. Conclusion

An improved ACSC-based harmonic current sharing control strategy for the paralleled VCIs in islanded MGs is proposed in this paper. In this sense, fast dynamic response and large stability margin can be endowed to the system. Moreover, the harmonic current among VCIs can be controlled independently. Current components at different sequences and orders are decomposed by a MSOGI-FLL. A HOVR is adopted to proportionally share the current outputs at different sequences and orders. Multiple PR controllers tuned at harmonic angular frequencies are used to suppress voltage harmonics. Simulation results validate the performance of the proposed control method.

References

[1] Xiongfei Wang, Frede Blaabjerg, Zhe Chen, "Autonomous Control of Inverter-Interfaced Distributed Generation Units for Harmonic Current Filtering and Resonance Damping in an Islanded Microgrid," IEEE Trans. Ind. Appl., vol. 50, no. 1, pp. 452–461, JAN./FEB. 2014.

[2] U. Borup, F. Blaabjerg, and P. Enjeti, "Sharing of nonlinear load in parallel-connected three-phase converters," IEEE Trans. Ind. Appl., vol. 37, no. 6, pp. 1817–1823, Nov./Dec. 2001.

[3] D. De and V. Ramanarayanan, "Decentralized parallel operation of inverters sharing unbalanced and non-linear loads," IEEE Trans. Power Electron., vol. 25, no. 12, pp. 3015–3025, Dec. 2010.

[4] Jinwei He, Yun Wei Li, Blaabjerg, F. "An Enhanced Islanding Microgrid Reactive Power, Imbalance Power, and Harmonic Power Sharing Scheme," IEEE Transactions on Power Electronics, vol. 30, no. 6, pp. 3389-3401, Jun. 2014.

[5] T. L. Lee and P. T. Cheng, "Design of a new cooperative harmonic filtering strategy for distributed generation interface converters in an islanding network," IEEE Trans. Power Electron., vol. 22, no. 5, pp. 1919–1927, Sep. 2007.

[6] P. T. Cheng, C. A. Chen, T. L. Lee, and S. Y. Kuo, "A cooperative imbalance compensation method for distributed-generation interface converters," IEEE Trans. Ind. Appl., vol. 45, no. 2, pp. 805–815, Mar./Apr. 2009.

[7] Jinwei He, YunWei Li, Josep M. Guerrero, Frede Blaabjerg, Juan C. Vasquez, "An Islanding Microgrid Power Sharing Approach Using Enhanced Virtual Impedance Control Scheme," IEEE Trans. Power Electron., vol. 28, no. 11, pp. 5272–5282, Sep. 2013.

[8] Tzung-Lin Lee, Po-Tai Cheng, "Design of a New Cooperative Harmonic Filtering Strategy for Distributed Generation Interface Converters in an Islanding Network," IEEE Trans. Power Electron., vol. 22, no. 5, pp. 1919–1927, Sep. 2007.

[9] Savaghebi, M., Jalilian, A., Vasquez, J.C., "Secondary Control for Voltage Quality Enhancement in Microgrids," Smart Grid, IEEE Transactions on, vol. 3, no. 4, pp. 1893-1902, Jul. 2012.

[10] Xiongfei W., Josep M. , Frede Blaabjerg, "Secondary voltage control for harmonics suppression in islanded microgrids," Power and Energy Society General Meeting, 2011 IEEE, Detroit, USA, 2011.

[11] Guan, Y., Guerrero, J.M., Zhao, X., Vasquez, J.C., Guo, X. "A New Way of Controlling Parallel-Connected Inverters by Using Synchronous-Reference-Frame Virtual Impedance Loop—Part I: Control Principle," Power Electronics, IEEE Transactions on, vol. 31, no. 6, pp: 4576 - 4593, June. 2016.